# Structural Changes and Biodegradation of PLLA, PCL, and PLGA Sponges During In Vitro Incubation

**Taiyo Yoshioka,[1] Fumiko Kamada,[1,2] Naoki Kawazoe,[1,3] Tetsuya Tateishi,[1] Guoping Chen[1,2,3]**
[1] *Biomaterials Center, National Institute for Materials Science, Tsukuba, Ibaraki 305-0044, Japan*

[2] *Graduate School of Pure and Applied Sciences, University of Tsukuba, Tsukuba, Ibaraki 305-0003, Japan*

[3] *International Center for Materials Nanoarchitectonics (MANA), National Institute for Materials Science, Tsukuba, Ibaraki 305-0044, Japan*

**The structural changes and degradation behaviors of poly(L-lactic acid) (PLLA) and poly(ε-caprolactone) (PCL) sponges were studied by incubation in phosphate buffer solution and compared with those of previously reported poly(lactic-*co*-glycolic acid) (PLGA) sponge. The changes of pH, weight, molecular weight, crystallinity, and thermal properties of glass transition and melting were measured. The influence of incubation temperature on the structural change of each type of sponge was investigated in details. During incubation, the PLLA sponge showed secondary crystallization, the PCL sponge showed lamellar thickening, and the PLGA sponge showed physical aging. Depending on the type of biodegradable polymers, the incubation temperature caused different structural changes during the incubation and the structural changes influenced several degradation behaviors. POLYM. ENG. SCI., 50:1895–1903, 2010. © 2010 Society of Plastics Engineers**

## INTRODUCTION

In tissue engineering, artificial scaffolds play an important role as templates to accommodate cells and guide the formation of new tissue [1, 2]. In successful scaffold design, the two main aspects that should be considered are structure and material. With reference to the structural aspect, it is generally required for the scaffolds to have a three-dimensional (3D) and highly interconnected porous structure with suitable mechanical properties, pore size, and porosity. As for the material aspect, in addition to acceptable biocompatibility, biodegradability is important. An ideal degradation behavior of scaffolds is having a degradation rate that matches the formation of new tissue or organs to enable gradual replacement of the scaffold with the proliferated cells and extracellular matrices [1–3]. In this sense, the degradation behavior of each material should be well understood in the process of material selection. To date, many kinds of synthetic and natural polymers have been extensively investigated as candidates for scaffold materials [4]. Among them, biodegradable aliphatic polyesters such as poly(ε-caprolactone) (PCL), poly(L-lactic acid) (PLLA), poly(glycolic acid) (PGA), and poly(lactic-*co*-glycolic acid) (PLGA) are the most desirable and widely used because of their versatile biodegradability.

The in vivo degradation of biodegradable aliphatic polyesters commonly undergoes a chemical hydrolysis reaction of ester bonds in its backbone [5]. Their degradability is affected by both the intrinsic properties of the polymer and the external environment. The polymer properties include monomer structure [6], molecular weight [7], copolymer ratio [8], crystallinity ($X_c$) [5, 9], shape [10], and glass transition temperature ($T_g$) [11], whereas the external environment includes pH [9, 12], temperature [13], and enzymes [14]. It is important to elucidate the structural changes of the porous scaffolds of the biodegradable polymers during in vitro incubation and their effect on the degradation of the scaffolds. The structural change is primarily dependent on the glass transition temperature of the biodegradable polymers and the incubation temperature. If $T_g$ of the crystalline polymer is below the incubation temperature of 37°C, further crystallization can be caused during the incubation period. If $T_g$ is near but above 37°C, physical aging (namely, enthalpy relaxation) of the amorphous part in either a crystalline or a noncrystalline polymer can occur during the incubation period. Both the structural changes in crystallization and physical

*Correspondence to*: G. Chen; e-mail: guoping.chen@nims.go.jp
Taiyo Yoshioka is currently at Material Sciences Center, Philipps University, Hans-Meerwein-Str, Marburg D-35032, Germany.
Contract grant sponsors: Ministry of Education, Culture, Sports, Science and Technology of Japan; contract grant sponsor: New Energy and Industrial Technology Development Organization of Japan.
DOI 10.1002/pen.21714
View this article online at wileyonlinelibrary.com.

aging during the incubation period can influence the degradation behavior of the polymer. The biodegradable polyesters, PLLA, PCL, and PLGA, have different crystallinities: $T_g$. PLLA is crystalline and its $T_g$ is above 37°C; PCL is crystalline and its $T_g$ is below 37°C; PLGA is noncrystalline and its $T_g$ is above 37°C. Therefore, the sponges of PLLA, PCL, and PLGA were used to investigate the relationship between structural change and their degradation. In this study, the structural changes and degradation behaviors of PLLA and PCL porous sponges in in vitro incubation were investigated and compared with those of PLGA, which has been reported previously [11].

## EXPERIMENTAL

### *Fabrication of Porous Sponges*

PLLA and PCL were purchased from Sigma-Aldrich (St. Louis, MO). The weight-average ($M_w$), number-average molecular weights ($M_n$), and polydispersity index (PDI) of PLLA measured by gel permeation chromatography (GPC) were 116,000 ± 4700, 65,700 ± 4100, and 1.77 ± 0.04, respectively. Those of PCL were 261,000 ± 2800, 165,000 ± 5000, and 1.60 ± 0.05, respectively. The PLLA and PCL sponges were fabricated by the particulate leaching technique using sieved sodium chloride (NaCl) particulates with a diameter range of 355–425 $\mu$m. Briefly, the NaCl particulates were added to each polymer solution in chloroform at a weight ratio of polymer/NaCl of 1/9 and mixed well. Then, the polymer/chloroform/NaCl mixture was poured immediately into a Teflon tube with an inside diameter of 10 mm. The chloroform was allowed to evaporate from both ends of the Teflon tube by air-drying for 1 day, and then the mixture was removed from the Teflon tube. The mixture was further dried in air for 1 day and in a vacuum for another 3 days. To leach out the NaCl particulates, the dried polymer/NaCl composite was immersed in deionized water that was changed every hour. The washing was continued until the weight of the dried sponge did not change. Finally, the complete leaching out of NaCl was confirmed by a simple qualitative analysis with a silver nitrate ($AgNO_3$) aqueous solution by which the change of transmittance caused by silver chloride precipitates of an ionic reaction product was detected by measuring light transmission. After drying, the resultant cylindrical sponges with diameters of 10 mm were cut into cylindrical specimen pieces having a height of 10 mm. NaCl, chloroform, and $AgNO_3$ solution were purchased from Wako Pure Chemical Industries (Osaka, Japan). Deionized water was obtained with a Milli-Q water filter system from Millipore Corporation (Bedford, MA).

Cross sections of the PLLA and PCL scaffolds were observed by a scanning electron microscope (SEM) (JSM-6400Fs, JEOL, Tokyo, Japan) operated at a voltage of 20 kV. The sponges were cut with a razor blade and then coated with platinum using a sputter coater (Sanyu Denshi, Tokyo, Japan). The pore size of each sponge was measured by analyzing the pore size of 10 randomly chosen SEM images of the cross sections.

### *In Vitro Degradation Test*

In vitro degradation tests of the PLLA and PCL scaffolds were conducted in phosphate buffer solution (PBS) under pH 7.4 at 37°C with mechanical shaking (60 shakes/min). PBS was prepared by mixing 18.2% (v/v) of 1/15 mol/l $KH_2PO_4$ aqueous solution and 81.8% (v/v) of 1/15 mol/l $Na_2HPO_4$ aqueous solution; the mixture solution was adjusted to pH 7.4. The PBS was autoclaved before use. Before the degradation test, each of the sponges was sterilized by 70% ethanol aqueous solution. This treatment served another important role as a pre-wetting treatment, which causes PBS to permeate into all of the pores of the sponges. After complete washing with sterile PBS, the sponges were immersed in 20 ml sterile PBS and 50 ml sterile glass test tubes were used as test vessels. To suppress pH change during the degradation test to a minimum, only the upper three-fourths of the PBS was replaced with fresh PBS every week [11]. After 6, 12, 18, and 26 weeks, the sponges were collected, washed with deionized water, air-dried for 1 day, and then vacuum-dried for another 3 days. The dried samples were used for various evaluations. The pH of the removed PBS was measured by a pH meter (Shimadzu, Kyoto, Japan).

### *Evaluation of Degraded Scaffolds*

The weights of the PLLA and PCL sponges were measured with an electrical balance, AG 135 (Mettler-Toledo International, NY). Weight loss in % was calculated according to a simple equation:

$$\text{Weight loss}(\%) = \frac{(W_0 - W_t)}{W_0} \times 100 \qquad (1)$$

where $W_0$ is the initial weight and $W_t$ is the weight at a given time. Both $W_0$ and $W_t$ were measured after vacuum drying for 3 days. $M_n$ of the PCL sponges and the peak top molecular weight of the PLLA sponges after a designed degradation time were determined by GPC using a high-performance liquid chromatography system, HLC-8220GPC (Tosoh, Tokyo, Japan), with two TSK gel columns ($GMH_{HR}$-M, Tosoh, Tokyo, Japan). Chloroform was used as the elution solvent at a flow rate of 1.0 ml/min at 40°C; TSK polystyrene standards (Tosoh, Tokyo, Japan) were used for calibration.

The melting temperature ($T_m$), $T_g$, and enthalpy of melting ($\Delta H_m$) of the PLLA and PCL sponges were determined by a differential scanning calorimeter (DSC), DSC8240 (Rigaku, Tokyo, Japan). A 5.0 mg of sample was analyzed from −30 to 250°C for PLLA sponge and from −100 to 150°C for PCL sponge at a rate of

 DOI 10.1002/pen

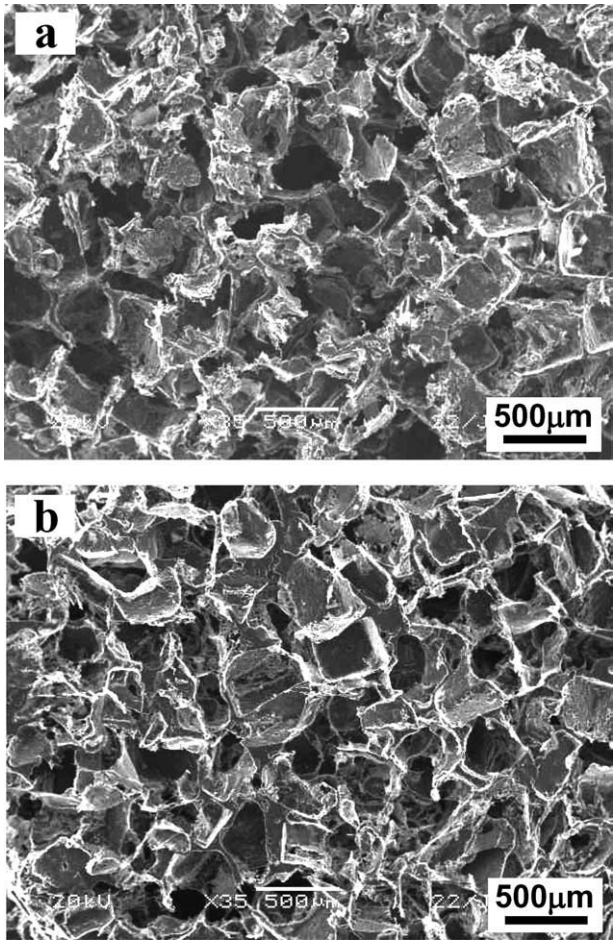


FIG. 1. SEM micrographs of cross sections of (a) PLLA and (b) PCL sponges.

10°C/min under a nitrogen gas flow at a rate of 50 ml/min. The instrument was calibrated with indium, tin, and lead. The $X_c$ of the sponges was evaluated according to the following equation:

$$X_c(\%) = \frac{\Delta H_m}{\Delta H_{m(\infty)}} \times 100 \quad (2)$$

where $\Delta H_{m(\infty)}$ is $\Delta H_m$ of a crystal having infinite crystal thickness. In this study, the $\Delta H_{m(\infty)}$ values of 93 and 140 J/g were used for PLLA and PCL, respectively [15, 16]. Ten samples at each time point were used for the weight and pH measurements. Three samples at each time point were used for GPC and DSC. The data were used to calculate the means and standard deviations.

## RESULTS AND DISCUSSION

### *PLLA and PCL Sponges*

The PLLA and PCL sponges were prepared by the particulate-leaching method. The typical images of the cross sections of the PLLA and PCL sponges are shown in Fig. 1a and b, respectively. Both the PLLA and PCL sponges had a highly porous structure, and each had an average pore size that was estimated to be 355.6 ± 73.0 $\mu$m and 363.9 ± 53.2 $\mu$m, respectively, values that are highly consistent with that of the NaCl particulates used.

### *Change of Weight*

Figure 2 shows the weight changes of the PLGA and PCL sponges with incubation time. The PLLA sponges showed a slight weight loss with incubation time, finally reaching a loss of up to 15.94% ± 2.88% after 26 weeks. In contrast, the PCL sponges showed almost no apparent weight loss (less than 1%) through the entire incubation period.

### *Change of Molecular Weight*

Figure 3a shows the GPC curves of the PLLA sponge with incubation time. In the first 6 weeks, a remarkable decrease in molecular weight and a characteristic peak deformation were observed simultaneously. In the peak deformation, three new specific peaks, which were numbered (1), (2), and (3) in turn from the low molecular weight side, appeared in addition to the original peak. The peak levels of peaks (1) and (2) both developed with incubation time; the development of peak (2) was more evident than that of peak (1). Peak (3) suddenly appeared at Week 18 and then almost disappeared. The change of the top molecular weight ($M_1$–$M_3$) of the peaks (1)–(3) is shown in Fig. 3b. The change of $M_1$ and $M_2$ showed a similar tendency in which the peak top molecular weight decreased slightly between Weeks 6–12 and 18–24, but changed only slightly during Weeks 12–18.

The GPC curves and change of $M_n$ of PCL with incubation time are shown in Fig. 4a and b, respectively. In contrast to the case of PLLA, no characteristic deformation of GPC curve was observed. $M_n$ remained unchanged for the first 6 weeks and then gradually decreased.

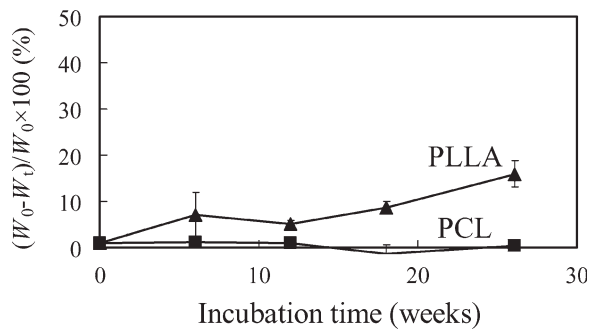


FIG. 2. Changes of weight loss (%) of PLLA and PCL sponges as a function of incubation time.

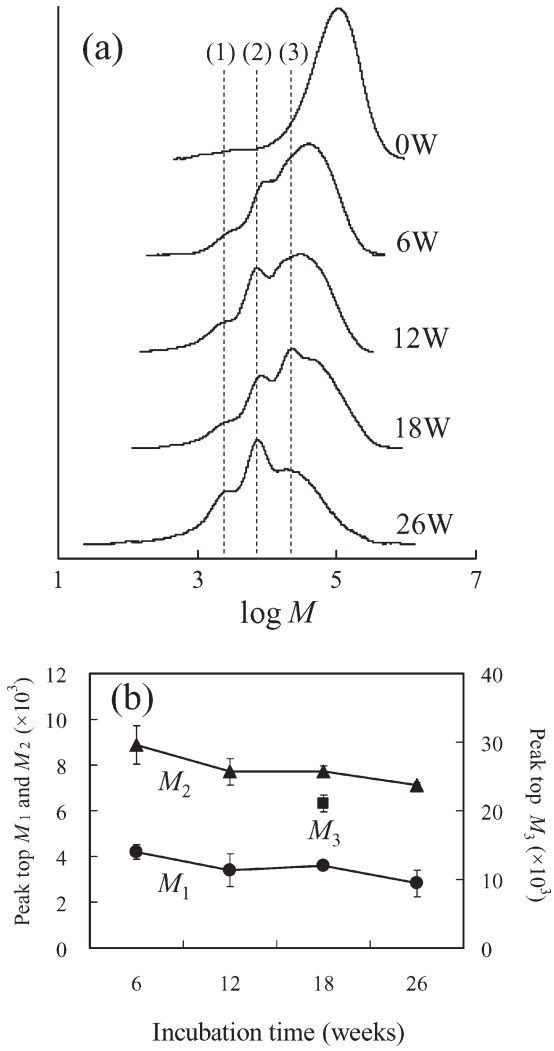


FIG. 3. (a) GPC curves in each incubation time of PLLA sponges and (b) changes of peak top molecular weights $M_1$, $M_2$, and $M_3$ for the specific peaks (1), (2), and (3) in (a) as a function of incubation time.

### *Change of Thermal Properties*

All the thermal properties for PLLA and PCL are discussed here without considering the influence of enthalpy relaxation because, in the preliminary experiments, it was confirmed that in both types the excess enthalpies of relaxation were negligibly small and always less than 1.0 J/g through the entire incubation period. Furthermore, no exothermal peak, which is related with the crystallization during heating process of DSC, was observed in this study for either sample of the PLLA and PCL sponges. The changes of $X_c$, $T_m$, and $T_g$ of the PLLA and PCL sponges with incubation time are shown in Fig. 5a–c, respectively. The initial $X_c$ of both the PLLA and PCL sponges were 59.6% and 56.5%, respectively.

For the first 12 weeks of incubation, $X_c$ of the PLLA sponges increased dramatically from 59.6 to 77.1%, and then showed no significant change. In contrast to $X_c$, $T_m$ of the PLLA sponges decreased for the first 12 weeks, and then showed no significant change. $T_g$ of the PLLA sponges increased for the first 12 weeks, especially during the first 6 weeks when it increased dramatically from 47 to 57.6°C. It decreased from 59.2 to 54.9°C during the next 6 weeks, and then showed no significant changes during the final 8 weeks.

$X_c$ of the PCL sponges increased for the first 12 weeks from 56.5 to 65.7%, and then showed no significant change. $T_m$ of the PCL sponges increased for the first 6 weeks, and then showed no significant change. $T_g$ of the PCL sponges remained almost unchanged throughout the incubation period.

### *pH Change of PBS*

In the hydrolysis reaction of biodegradable polyesters, acidic degradation products, which act as a catalysis of the following hydrolysis reaction, are generated. Therefore, if the reaction system is not changed during the course of the hydrolysis reaction, the pH of the system becomes acidic as the reaction proceeds, especially under neutral conditions. In an in vivo environment, the influ-

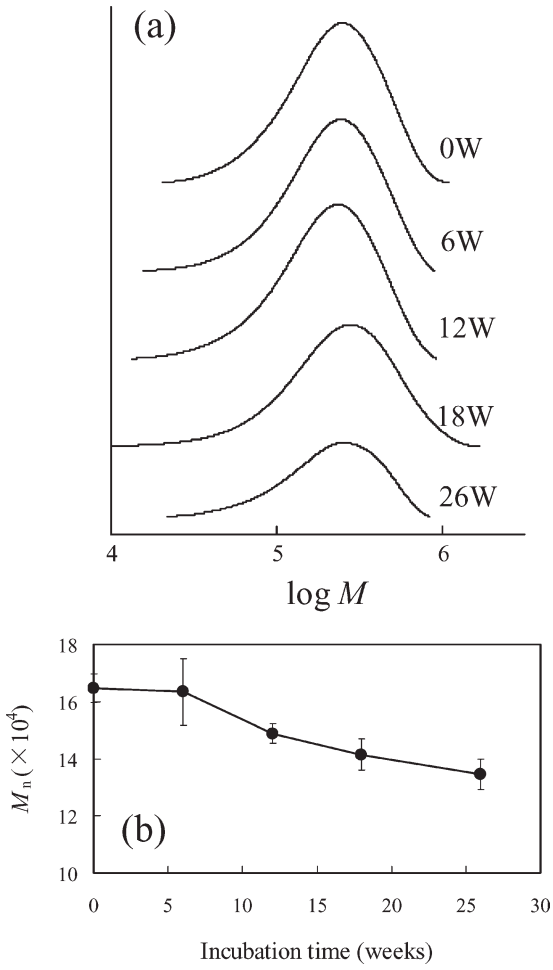


FIG. 4. (a) GPC curves in each incubation time of PCL sponges and (b) change of number-averaged molecular weight ($M_n$).


DOI 10.1002/pen

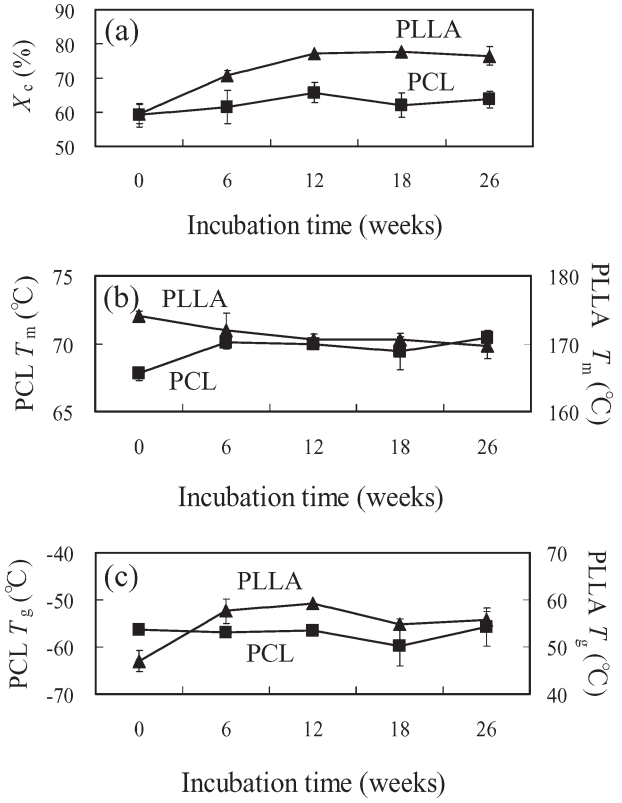


FIG. 5. Changes of (a) crystallinity ($X_c$), (b) melting temperature ($T_m$), and (c) glass transition temperature ($T_g$) as a function of incubation time of PLLA and PCL sponges.

ence of acidic products on pH should be suppressed by the native buffer and circulation systems. In contrast, normally in in vitro studies, the influence of acidic products is partially or completely suppressed by using the following methods in part or completely: (1) by using a buffer solution, (2) by regularly changing the buffer solution completely, (3) by mildly agitating the incubation system. In our previous report, a new protocol was proposed to suppress the extreme pH change in which the incubation test was done under a mild shaking condition and three-fourths of the PBS was regularly changed [11]. In this study, we used the same protocol to suppress extreme pH change. The resultant pH change of PBS in the case of both the PLLA and PCL sponges was suppressed within 7.33–7.37 and 7.33–7.38, respectively, throughout the entire incubation period.

### *Degradation Behavior of PLLA Sponges*

For convenience, the changes in pH, $M_n$, weight, $X_c$, $T_m$, and $T_g$ of the PLLA sponges with incubation time are schematically depicted in Fig. 6. In the graph, each change is depicted with a simplified and characterized line and is not quantitative.

As a characteristic change, $X_c$ increased, however, $M_n$, weight, and $T_m$ decreased for the first 12 weeks. The decrease of $M_n$ and weight for the first 12 weeks could be

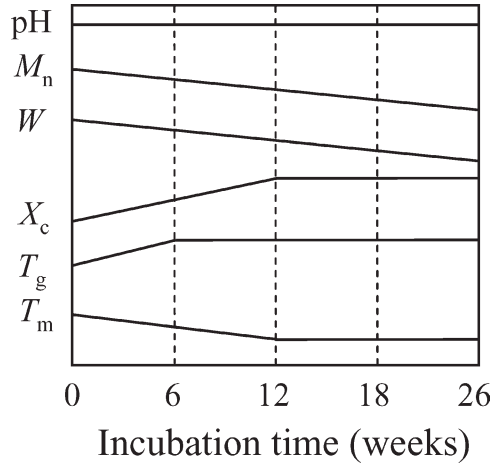


FIG. 6. Schematic graph of changes in pH, $M_n$, weight ($W$), $X_c$, $T_m$, and $T_g$ for PLLA sponges. Each change is depicted with a simplified and characterized line and is not quantitative.

attributed partly to the preferential degradation and release of the amorphous part of the PLLA sponge because it is well known that water molecules can diffuse more easily into the amorphous part than they do into the crystalline part. A supporting image is shown in Fig. 7. Figure 7 is an SEM image of a pore wall of a fractured PLLA sponge that was treated with a 0.5 N sodium hydroxide aqueous solution (NaOHaq) at 37°C for 1 h. By the alkaline treatment, closely filled crystalline spherulites composed of radially grown ribbon-like crystalline lamellae were revealed, demonstrating the preferential removal of the amorphous part by the NaOHaq treatment. Many "∞"-like shaped twin halls in the image, some of which are surrounded with white lines, seem to correspond to the spherulite centers that are composed of less organized structures

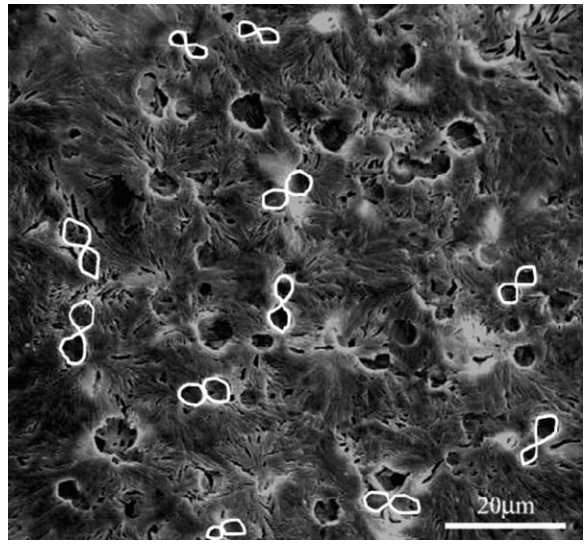


FIG. 7. SEM micrograph of a pore surface of an alkaline-etched PLLA sponge with 0.5 N NaOH aq at 37°C for 1 h. Some of the typical pairs of twin halls with a "∞"-like shape, which are thought to be spherulite centers, are surrounded with white dashed lines.

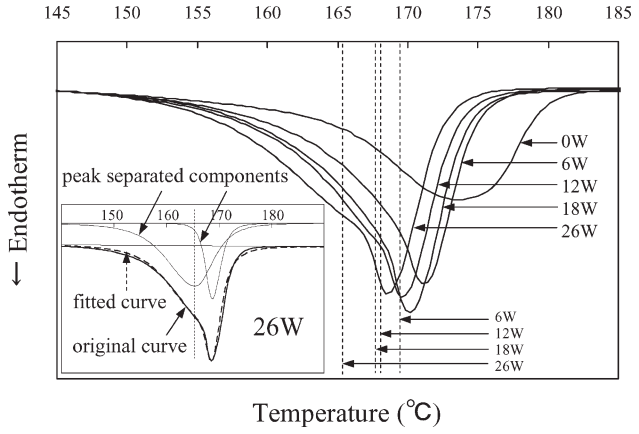


FIG. 8. DSC curves for melting of PLLA sponges during each incubation time. The inset shows an example of the peak separation process. The broken straight lines show the peak top positions of each lower side peak component.

and, therefore, susceptible to alkaline etching [17–19]. Considering that the incubation condition in this study was milder than that of the NaOHaq treatment, the preferential degradation and release of the amorphous part of the PLLA sponges should occur during incubation in PBS. Except for the preferential degradation of the amorphous part, however, there should also be other factors affecting $X_c$ because the $X_c$ calculated from weight loss was lower than the experimentally obtained $X_c$. Assuming that the weight loss is attributed to only the amorphous part, the resultant $X_{c(t)}$ in each incubation time can be calculated by $100 \times X_c/[100-\text{weight loss (\%)}]$ (namely $= X_c W_0/W_t$) because the $X_c$ obtained from the DSC is given as a mass fraction crystallinity. The calculated $X_c$ of the PLLA sponge, for example, after Weeks 12 and 26 of incubation was 62.9% and 70.9%, respectively. However, the measured $X_c$ after Weeks 12 and 26 incubation was 77.1% and 76.5%, respectively. The results indicate that formation of new crystals (namely, secondary crystallization) might occur during incubation. Secondary crystallization during incubation is also demonstrated from the change of the shape of the melting peak. The DSC curves for melting of the PLLA sponges during each incubation time are shown in Fig. 8. A specific change of peak type from single to double peak occurred after incubation. All the melting peaks after incubation can be well divided by a peak separation technique into two different peaks of a higher temperature side with a narrower half-width at half-maximum (HWHM) and of a lower temperature side with a broader HWHM. In principle, the shape of the melting peak on DSC curves is not symmetrical [20] and, therefore, the asymmetric Gaussian distribution function in the free software "Fityk ver. 0.8.6" was used in this study according to the DSC peak separation technique by Netzsch Corp [21]. An example of peak separation for Week 26 is shown as an inset in Fig. 8. The straight broken lines in Fig. 8 show the peak top positions of each lower side peak component. Because the peak area of the broader curves at low temperature side was always larger than that at high temperature side, it is reasonable, but not unquestionable, to consider that the lower temperature side are attributed to the melting of the original lamellae, and that the narrower curves of the higher temperature side are the new lamellae. The Thompson-Gibbs equation (*Eq. 3* and also expressed as *Eq. 4*) shows that $L_c$ of the new crystals ($L_{nc}$) is slightly thicker than that of the original crystals ($L_{oc}$), where $T_m^0$, $\sigma$, $\Delta h^0$, and $\rho_c$ in *Eq. 3* are the equilibrium $T_m$, specific fold surface free energy, heat of fusion (per unit mass), and crystal density, respectively. This tendency is the opposite to that of a report by Zong et al. on the secondary crystallization of PGA and PLGA during incubation [22]. Tsuji and Ikada investigated the relationship between $T_m$ and $L_c$ in PLLA film, and determined the values of $T_m^0$ and $2\sigma/\Delta h^0 \rho_c$ as 198°C and 1.59°C, respectively [15]. Using their values and experimentally obtained $T_m$, the $L_c$ values [$L_{c(Tm)}$] during each incubation time were estimated from *Eq. 4* and listed in Table 1. Here, the values estimated from the lower temperature side components in each peak of the separated curves were used as $T_m$.

$$T_m = T_m^0 \left[1 - \frac{2\sigma}{\Delta h^0 \rho_c L_c}\right] \tag{3}$$

$$L_c = \frac{2\sigma T_m^0}{\Delta h^0 \rho_c (T_m^0 - T_m)} \tag{4}$$

Three specific low molecular weight peaks were observed in the GPC curves (Fig. 3a). Similar results in PLLA films were reported by Fischer et al. [17] and by Tsuji and Ikada [15]. Such specific peaks were ascribed to the generation of some specific molecular weight fractions due to the degradation of folding chain parts in the lamellar crystals. It is known that PLLA crystallizes with α-modification under static conditions. The crystal structure was determined by Hoogsteen et al. to be a pseudo-orthorhombic structure ($a = 1.07$, $b = 0.595$, and $c$ (chain axis) $= 2.78$ nm) composed of two chains having a left-handed 10/3 helix conformation [23]. Assuming that $M_1$ is attributed to $L_c$ in each incubation time, the $L_c$ values [$L_{c(M1)}$] expected from $M_1$ can be estimated by the equation:

$$L_{c(M_1)}(\text{nm}) = \frac{0.278 \times M_1}{72.1} \tag{5}$$

where 0.278 and 72.1 are the length occupied by one lactide monomer unit in the $c$-axis direction in the crystal

TABLE 1. Estimated values of PLLA lamellar thickness from the $T_m$ [$L_{c(Tm)}$] and the peak top $M_1$ [$L_{c(M1)}$].

| Incubation time/weeks | 0 | 6 | 12 | 18 | 26 |
|---|---|---|---|---|---|
| $L_{c(Tm)}$/nm | 13.1 | 11.1 | 10.5 | 10.4 | 9.7 |
| $L_{c(M1)}$/nm | — | 16.2 | 13.1 | 13.9 | 10.9 |


DOI 10.1002/pen

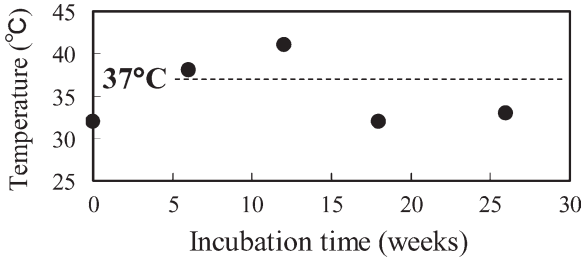


FIG. 9. Change of onset temperature of glass transition in PLLA sponges as a function of incubation time.

and the lactide monomer mass per mole, respectively. Table 1 lists the estimated $L_{c(M1)}$ values in each incubation time. The good similarity of the values between $L_{c(M1)}$ and $L_{c(Tm)}$ clearly supports the initial assumption, although the difference in Week 6 is somewhat large compared with the other incubation times. Probably, such a difference in the beginning of incubation arises from the inevitable contribution of the noncrystalline chain ends to $L_{c(M1)}$, which was based on the chain folding part. The values of $M_2/M_1$ in each incubation time were calculated to be 2.11, 2.26, 2.14, and 2.52 for Weeks 6, 12, 18, and 24, respectively. These values of $\sim$2 agree well with the idea that peak (2) is ascribed to the one-folded chains (namely, to the $2L_c$ + one-folding chain part). The reason the values are always slightly over 2 could be attributed partly to the extra folding chain part in the one-folded chains. The value of $M_3/M_1$ at Week 18 was calculated to be 5.83. This shows that peak (3) is not ascribed to the two-folded chains but to the four-folded chains (namely, the $5L_c$ + four-folding chain parts). In Fig. 3a, the additional independent peaks corresponding to $L_{nc}$ are not seen. This is probably because the thicknesses of $L_{nc}$ and $L_{oc}$ are too close. On the other hand, the Thompson-Gibbs equation suggests that $L_c$ had started to decrease during the first 6 weeks. It is not easy to accept this, however, because the GPC results demonstrated that many folding chain parts still remained in Week 26. Thus, it is speculated that the decrease of $T_m$ during the beginning of incubation was not primarily caused by the decrease of $L_c$ but probably by the increase of $\sigma$ due to the scission of the folding chain part.

Here, it should be contemplated as to why the PLLA, having its $T_g$ of 47°C, was able to crystallize during incubation at 37°C. It is well known that polymer has a rather broad glass transition range and that $T_g$ is influenced by various parameters such as free volume, conformational entropy, and molecular weight of amorphous chains. Figure 9 shows the onset temperatures of glass transition in the DSC results for each incubation time. The figure indicates that the amorphous molecules, which can crystallize during incubation at 37°C, existed in the intact PLLA sponges, and the increases of $T_g$ and the onset temperature of glass transition for the first 6 weeks are caused by the crystallization of such amorphous chains. Tsuji and Ikada have proposed that the amorphous region between the stacked lamellae should include many molecular level voids due to the existence of tie chains and folding chain parts [15]. On the other hand, it is well known that during the formation of polymer spherulites, low molecular weight species are rejected from the crystallization and the chains tend to be segregated primarily between the stacked lamellae [24, 25]. From these points, it is believed that the amorphous chains, existing between the stacked lamellae, are energetically less stable than the others existing between the adjacent lamellae or the spherulite boundaries. Thus, the thermal motion of these unstable chains should be initiated at a lower temperature compared with the others. In addition, Hu et al. proposed that a pre-aligned single chain, having low conformational entropy, could behave as a nucleus of the subsequent epitaxial crystallization process [26]. Therefore, it is speculated that the secondary crystallization during incubation mostly occurs between the stacked lamellae, and the thermodynamic driving force was the low conformational entropy of the nearly extended tie chains between stacked lamellae. This speculation suitably explains why the secondary crystallization occurred at only the beginning of incubation during which a large amount of tie chains still remains. In addition, this speculation also acceptably explains the experimental results of Zong et al. on the secondary crystallization of PGA and PLGA during incubation, i.e., that the new crystals formed in parallel with the original stacked lamellae [22]. In Week 18, the onset temperature of glass transition again decreased to around 30°C. This might be due to the progress of degradation of the remaining amorphous chains. However, such newly generated unstable amorphous chains were no longer able to crystallize because of the lack of tie chains.

### *Degradation Behavior of PCL Sponges*

The changes in pH, $M_n$, weight, $X_c$, $T_m$, and $T_g$ of the PCL sponges with incubation time are schematically depicted in Fig. 10. It is well known that the degradation rate of PCL sponges under pH 7.4 at 37°C is considerably slower than that of PLLA sponges [4]. In addition, in this study, during the incubation period of 26 weeks, weight loss was not recognized and only a gradual decrease in $M_n$ was recognized after 6 weeks. In contrast, as a characteristic change, $X_c$ and $T_m$ increased for the first 6 weeks without any changes of $M_n$ and weight. Because $T_g$ of intact sponge is $-56.3$°C, at the incubation temperature of 37°C the amorphous chains are in a rubber-like state and, therefore, able to crystallize. Simultaneously, the incubation temperature should act as an annealing temperature for the original crystals. Thus, the following three cases must be considered as explanations of the increases of $X_c$ and $T_m$ for the first 6 weeks: (1) new lamellar crystals having thicker $L_{nc}$ than $L_{oc}$ formed, (2) lamellar thickening of the original crystals occurred, or (3) both cases (1 and 2) occurred simultaneously. However, taking into account that the additional melting peak in the DSC curve

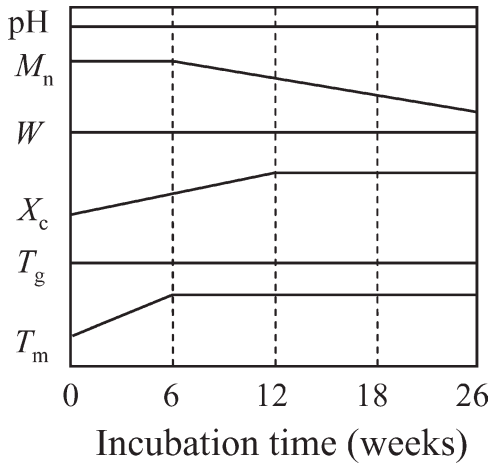


FIG. 10. Schematic graphs of changes in pH, $M_n$, weight ($W$), $X_c$, $T_m$, and $T_g$ for PCL sponges. Each change is depicted with a simplified and characterized line and is not quantitative.

did not appear during every incubation period, possibilities (1) and (3) are not acceptable. Using Eq. *4*, based on values in the literature of $T_m^0 = 70.5°C$ [27, 28], $\sigma = 90$ mJ/m$^2$ [27, 28], $\Delta h^0 = 135$ J/g [28], and $\rho_c = 1.20$ g/cm$^3$ [29], the $L_c$ values at Weeks 0 and 6 are estimated to be 29 and 157 nm, respectively. The lamellar thickness increased for the first 6 weeks by about five times. The lamellar thickening of PCL was well investigated by Phillips and Rensch [30]. They proposed a similar lamellar thickening model with one for polyethylene where crystal thickening occurred by combining several original folded-chain crystals stacked up and down through chain sliding diffusion [31, 32]. The resultant new folded-chain crystal has a thickness of integral multiples of $L_{oc}$, ultimately leading to formation of an extended-chain crystal. When the lamellar thickening occurs by combining several original crystals through chain sliding diffusion, the amorphous regions between each original crystal are converted into crystalline regions. Therefore, it is reasonable to increase the $X_c$ accompanied by the lamellar thickening for the first 6 weeks. However, this cannot explain the further increase of $X_c$ from Weeks 6 to 12. This increase of $X_c$ without the accompanying $T_m$ change indicates that new crystallization occurred. As mentioned above, because the new melting peak in the DSC curve was not observed throughout, it can be assumed that new crystallization occurred epitaxially on the side of the thickened lamellar crystals with the same lamellar thickness. The degradation of the amorphous chains might promote the epitaxial overgrowth.

### *Comparison of Degradation Behaviors of PLLA, PCL, and PLGA Sponges*

In addition to the PLLA and PCL sponges, we have already investigated and reported the degradation behavior of noncrystalline PLGA sponges using the same protocol used in this report, except for sponge shape. The PLGA sponges degraded more rapidly than did the PLLA and PCL sponges, and the weight loss of the PLGA sponges reached about 80% for incubation of 24 weeks. Generally, in hydrolytic degradation of aliphatic biodegradable polyesters under neutral or basic conditions, the higher electrophilicity of carbonyl carbon atoms leads to greater susceptibility to attack by hydroxide ions [6]. Following this, the order of degradability can be expected as PLGA > PLLA > PCL. This order has also been widely confirmed in the sponge forms. However, it is also well known that the degradability and especially the degradation behavior are not determined by only the chemical structure but also by the primary, secondary, and tertiary structures of the materials. In the previous study on noncrystalline PLGA, we clarified that the degradation mechanism during the first 12 weeks is mostly based on autocatalyzed bulk degradation and, after Week 12, the dominant degradation mechanism changes into surface degradation. In other words, the degradation behavior of the first 12 weeks was explained very well with a well known equation for autocatalyzed bulk degradation, $\ln M_n(t) = \ln M_n(0) - k_t$. This equation is derived from the basic kinetics of the hydrolysis reaction based on chemical structure [33]. On the other hand, in this study, the changes of $M_n$ with the incubation time of the crystalline PLLA sponges showed a more complex behavior, which was strongly influenced by crystal thickness, which corresponds to the secondary structure. In addition, formation of new crystals during incubation was confirmed. It is no doubt that the newly formed crystalline entities also influence the degradation behavior.

In the evaluation of the degradation behavior of these three kinds of sponges, the importance of the relationship between $T_g$ and incubation temperature is clear. In the case of noncrystalline PLGA sponges, whose $T_g$ is above but near the incubation temperature, it was confirmed that physical aging occurred during incubation and that the heterogeneous structure caused by the physical aging might be one of the driving forces to induce autocatalyzed bulk degradation. In contrast, in the case of the crystalline PLLA and PCL sponges, the incubation temperature acted on each crystalline morphology with completely different effects and, as a result, secondary crystallization and lamellar thickening were observed in the PLLA and PCL sponges, respectively. The most important information resulting from this study is that in each of the PLLA, PCL, and PLGA materials structural changes caused by incubation temperature occurred and completed during the beginning of incubation, which is considered the most important period for cell adhesion, proliferation, and differentiation.

## CONCLUSIONS

The structural changes and degradation behaviors of PLLA and PCL sponges were investigated by incubating

 DOI 10.1002/pen

both sponges in PBS at pH 7.4 and 37.0°C under mild shaking with three-fourths of the PBS being changed every week. The PLLA sponges showed molecular weight fractionation for the first 12 weeks, and the dominant fractions were the non- and one-folded chains. At the same time, secondary crystallization also occurred. Molecular weight fractionation proceeded from Weeks 12 to 26, and the four times folded chains appeared as the dominant fractions in addition to the non- and one-folded chains. Secondary crystallization was no longer observed. The PCL sponges showed lamellar thickening of the original crystals during the first 6 weeks by combining several original lamellar crystals stacked up and down through the chain sliding diffusion. Epitaxial overgrowth of new crystalline domain occurred in the thickened lamellar crystals from Weeks 6 to 12, and degradation of the amorphous chains started. Degradation of the amorphous chains proceeded gradually from Weeks 12 to 26. These attributes of PLLA and PCL were compared with those of PLGA sponge, which has been reported previously. It was shown that the incubation temperature caused different types of structural changes during incubation and that the structural changes influenced several degradation behaviors. Structural changes such as secondary crystallization in PLLA sponge, lamellar thickening in PCL sponge, and physical aging in PLGA sponge occurred and completed during the beginning of incubation.

## REFERENCES


1. R. Langer and J.P. Vacanti, *Science*, **260**, 920 (1993).
2. G. Chen, T. Ushida, and T. Tateishi, *Macromol. Biosci.*, **2**, 67 (2002).
3. S. Yang, F.E. Leong, Z. Du, and C.K. Chua, *Tissue Eng.*, **7**, 679 (2001).
4. L.S. Nair and C.T. Laurencin, *Prog. Polym. Sci.*, **32**, 762 (2007).
5. S.C.J. Loo, C.P. Ooi, S.H.E. Wee, and Y.C.F. Boey, *Biomaterials*, **26**, 2827 (2005).
6. J.H. Jung, M. Ree, and H. Kim, *Catal. Today*, **15**, 283 (2006).
7. S.K. Saha and H. Tsuji, *Mater. Eng.*, **291**, 357 (2006).
8. T.G. Park, *Biomaterials*, **16**, 1123 (1995).
9. H. Tsuji, Y. Tezuka, and K. Yamada, *J. Polym. Sci. Polym. Phys.*, **43**, 1064 (2005).
10. K.H. Lam, P. Nieuwenhuis, and I. Molenaar, *J. Mater. Sci. Mater. Med.*, **5**, 181 (1994).
11. T. Yoshioka, N. Kawazoe, T. Tateishi, and G. Chen, *Biomaterials*, **29**, 3438 (2008).
12. C.E. Holy, S.M. Dang, J.E. Davies, and M.S. Shoichet, *Biomaterials*, **20**, 1177 (1999).
13. A.C.M. Grayson, M.J. Cima, and R. Langer, *Biomaterials*, **26**, 2137 (2005).
14. H. Tsuji and Y. Tezuka, *Macromol. Biosci.*, **5**, 135 (2005).
15. H. Tsuji and Y. Ikada, *Polym. Degrad. Stab.*, **67**, 179 (2000).
16. Q. Meng, J. Hu, Y. Zhu, J. Lu, and Y. Liu, *Smart. Mater. Struct.*, **16**, 1192 (2007).
17. E.W. Fischer, H.J. Sterzel, and G. Wegner, *Kolloid-ZZ Polym.*, **251**, 980 (1973).
18. Y. He, Z. Fan, Y. Hu, T. Wu, J. Wei, and S. Li, *Eur. Polym. J.*, **43**, 4431 (2007).
19. Y. Kikkawa, H. Abe, M. Fujita, T. Iwata, Y. Inoue, and Y. Doi, *Macromol. Chem. Phys.*, **204**, 1822 (2003).
20. S. Fujieda and R. Uchida, *Anal. Sci.*, **9**, 701 (1993).
21. X. Qin, J. Qu, and X. Cao, *Polym. Bull.*, **56**, 607 (2006).
22. X.H. Zong, Z.G. Wang, B.S. Hsiao, B. Chu, J.J. Zhou, D.D. Jamiolkowski, E. Muse, and E. Dormier, *Macromolecules*, **32**, 8107 (1999).
23. W. Hoogsteen, A.R. Postema, A.J. Pennings, G. Brinke, and P. Zugenmaier, *Macromolecules*, **23**, 634 (1999).
24. W. Hu, *Macromolecules*, **38**, 8712 (2005).
25. A. Mebta and B. Wunderlich, *Colloid. Polym. Sci.*, **253**, 193 (1975).
26. W. Hu, D. Frenkel, and V.B.F. Mathot, *Macromolecules*, **35**, 7172 (2002).
27. P.J. Phillips, G.J. Rensch, and K.D. Taylor, *J. Polym. Sci. Part B: Polym. Phys.*, **25**, 1725 (1987).
28. E. Nunez, C. Ferrando, E. Malmstrom, H. Claesson, P.E. Werner, and U.W. Gedde, *Polymer*, **45**, 5251 (2004).
29. Y. Chatani, Y. Okita, H. Tadokoro, and Y. Yamashita, *Polym. J.*, **1**, 555 (1970).
30. P.J. Phillips and G.J. Rensch, *J. Polym. Sci. Part B: Polym. Phys.*, **27**, 155 (1989).
31. M. Hikosaka, K. Amano, S. Rastogi, and A. Keller, *J. Mater. Sci.*, **35**, 5157 (2000).
32. P.J. Barham and A. Keller, *J. Polym. Sci. Part B: Polym. Phys.*, **27**, 1029 (1989).
33. A.C. Renouf-Glauser, J. Rose, D. Farrar, and R.E. Cameron, *Biomaterials*, **26**, 2415 (2005).